Novel multifunctional PHDCA/PEI nano-drug carriers for simultaneous magnetically targeted cancer therapy and diagnosis via magnetic resonance imaging

2007 Nanotechnology 18 475105

(http://iopscience.iop.org/0957-4484/18/47/475105)

Nanotechnology **18** (2007) 475105 (8pp) doi:10.1088/0957-4484/18/47/475105

Novel multifunctional PHDCA/PEI nano-drug carriers for simultaneous magnetically targeted cancer therapy and diagnosis via magnetic resonance imaging

Sung-Baek Seo[1,2], Jaemoon Yang[2], Woochan Hyung[2], Eun-Jin Cho[1,3], Tong-Il Lee[4], Yong Jin Song[5], Ho-Geun Yoon[6], Jin-Suck Suh[1,3], Yong-Min Huh[1,3,7] and Seungjoo Haam[1,2,7]

[1] Graduate Program for Nanomedical Science, Yonsei University, Seoul 120-749, Korea
[2] Department of Chemical Engineering, College of Engineering, Yonsei University, Seoul 120-749, Korea
[3] Department of Radiology, College of Medicine, Yonsei University, Seoul 120-752, Korea
[4] ATGen, Advanced Technology Research Center, 68 Yatap-dong, Bundang-gu, Seongnam-si, Gyeonggi-do, 463-816, Korea
[5] Department of Physics, College of Natural Science, Ajou University, Suwon 433-749, Korea
[6] Department of Biochemistry and Molecular Biology, Center for Chronic Metabolic Disease Research, College of Medicine, Yonsei University, Seoul 120-752, Korea

E-mail: ssjjy8199@yonsei.ac.kr (S-B Seo), 177hum@yonsei.ac.kr (J Yang), afkiller@yonsei.ac.kr (W Hyung), ejc@yumc.yonsei.ac.kr (E-J Cho), singout72@atgen.co.kr (T-I Lee), yjsong@ajou.ac.kr (Y J Song), yhgeun@yumc.yonsei.ac.kr (H-G Yoon), jss@yumc.yonsei.ac.kr (J-S Suh), ymhuh@yumc.yonsei.ac.kr (Y-M Huh) and haam@yonsei.ac.kr (S Haam)

Received 25 April 2007, in final form 2 October 2007
Published 26 October 2007
Online at stacks.iop.org/Nano/18/475105

Abstract
Novel multifunctional magnetic polycation drug carriers (MPDCs) were synthesized to provide simultaneous magnetically targeted cancer therapy and diagnosis via magnetic resonance imaging (MRI). The MPDCs consist of ultra-sensitive magnetic nanocrystals as MR probes and for magnetic targeting, and a chemotherapeutic agent encapsulated in poly(hexadecylcyanoacrylate) (PHDCA) nanoparticles. The PHDCA nanoparticles were further coated with polycationic polyethylenimine (PEI) to enhance cellular uptake efficiency. The MPDCs demonstrated ultra-sensitivity via MRI and sufficient magnetic mobility under an external magnetic field. Drug loading efficiency and release kinetics were also investigated. From the cell viability data, the MPDCs were nontoxic and the doxorubicin hydrochloride (DOX)-loaded MPDCs exhibited excellent tumorcidal efficacy.

1. Introduction

The application of multifunctional nanocomplexes to the field of oncology has offered innovative solutions to early cancer detection, *in vivo* tumor imaging, personalized diagnostics and targeted therapeutics [1–4]. Recently, cancer treatment using polymeric drug carriers has been considered because of their biodegradability, low cytotoxicity and the ability to control drug release kinetics [5]. Various methods for the delivery of anti-cancer drugs to specific tumor sites using polymeric drug carriers have been extensively studied with the aim of reducing side effects and increasing drug efficacy. Antigen–antibody interactions, pH, temperature and magnetic field have been widely used as targeting moieties [6]. Among these, noninvasive targeted drug delivery to cancer cells, using an external magnetic field, has been applied to local areas of various types of cancer [7–9].

[7] Authors to whom any correspondence should be addressed.

Magnetic nanoparticles can be used as excellent magnetic resonance imaging (MRI) probes for noninvasive *in vivo* monitoring of molecular and cellular events. For example, we developed ultra-sensitive MR probe systems based on magnetism-engineered iron oxide nanoparticles. These considerably enhanced the sensitivity of cancer detection to enable *in vivo* imaging of small volume tumors at an early stage [10]. Furthermore, we recognized that imaging agents and anti-cancer drugs could be colocalized to specific tumor sites using polymeric drug carriers through the application of a noninvasive external magnetic field to allow simultaneous treatment and diagnosis. This enables us to regulate the amount of anti-cancer drug injected through real-time monitoring of tumor volume by MRI. Moreover, simultaneous treatment and diagnosis will improve the therapeutic outcome of cancer chemotherapy and result in improved patient compliance and comfort compared with the two-step cancer treatment of surgery or chemotherapy followed by detection of tumor volume change.

In this study, we focused on formulation and characterization of multifunctional magnetic polycation drug carriers (MPDCs) for simultaneous magnetically targeted cancer therapy and diagnosis at the cellular level for a proof of concept, as in our previous study [11]. The MPDCs contain ultra-sensitive magnetic nanocrystals as MR probes and for magnetic targeting, and doxorubicin hydrochloride (DOX) as an anti-cancer drug encapsulated in poly(hexadecylcyanoacrylate) (PHDCA) nanoparticles. As MR and magnetic targeting probes, the monodispersed magnetic nanocrystals were synthesized in organic solvent [12]. The PHDCA nanoparticles exhibited relatively rapid degradability in the early stage, which is critical in magnetically targeted cancer therapy [13]. To achieve stability in the aqueous phase, magnetic PHDCA nanoparticles (MPNs) were prepared in a spherical form by stabilizers using the emulsion solvent evaporation method. Moreover, cellular uptake can be increased by cationic polymers such as polyethylenimine (PEI), poly(L-lysine), and chitosan, that can easily associate with negatively charged cell membranes through electrostatic interactions and are internalized into cancer cells by charge-mediated endocytosis [14–17]. Therefore, the anionic MPNs were further coated with polycationic PEI to enhance cellular uptake efficiency through ionic interactions, yielding PEI/MPNs nanocomplexes (MPDCs) (figure 1). The magnetic mobility of the MPDCs under an external magnetic field was observed using epi-fluorescence microscopy. The diagnostic potential of the MPDCs as magnetic resonance contrast agents was demonstrated by MRI. Finally, to assess the therapeutic potential of the MPDCs, we investigated drug release kinetics and cell viability using MTT [3-(4,5-dimethylthiazol-2-yl)-2,5-diphenyltetrazolium bromide] assay.

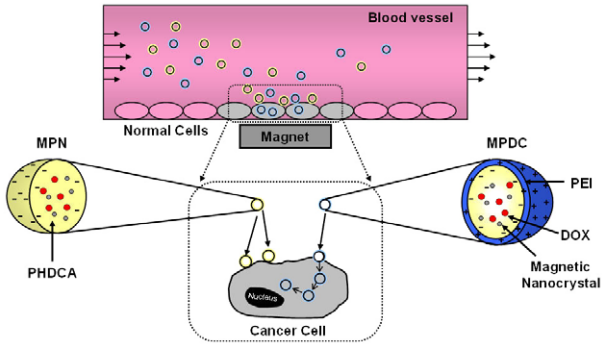

Figure 1. Conceptual scheme of multifunctional magnetic polycation drug carriers (MPDCs). The MPDCs enable drug delivery to targeted sites using an external magnetic field and can simultaneously be used as magnetic resonance contrast agents for local detection. The MPDCs also possess enhanced cellular uptake efficiency and therapeutic efficacy compared with MPNs due to their surface characteristics. The outermost polycationic PEI of the MPDCs allows electrostatic interactions with negatively charged cell membranes, followed by internalization into cancer cells.

2. Materials and methods

2.1. Materials

Iron(III) acetylacetonate, 1,2-hexadecanediol, dodecanoic acid, dodecylamine, benzyl ether, hexadecanol, cyanoacetic acid, 1,4-dimethylaminopyridine, 1,3-dicyclohexylcarbodiimide, anhydrous dichloromethane, dimethylamine, polyethylenimine (PEI, M_w: 25k), polyvinyl alcohol (PVA, M_w: 15–20 kilo.) and rhodamine B were purchased from Sigma-Aldrich. Doxorubicin hydrochloride (DOX) and fluorescein isothiocyanate (FITC) were obtained from Fluka. Phosphate buffered saline (PBS; 10 mM, pH 7.4) was purchased from Gibco. All other chemicals and reagents were of analytical grade.

2.2. Synthesis of magnetic nanocrystals

2 mM of iron (III) acetylacetonate, 10 mM of 1,2-hexadecanediol, 6 mM of dodecanoic acid, 6 mM of dodecylamine and benzyl ether (20 ml) were mixed under ambient nitrogen. The mixture was preheated to 150 °C for 30 min and then refluxed at 300 °C for 30 min. After cooling to room temperature, the products were purified with an excess of pure ethanol. Magnetic nanocrystals of ∼10 nm diameter were synthesized using the seed-mediated growth method [12].

2.3. Synthesis of HDCA monomers and PHDCA

Hexadecylcyanoacetate (HDCA) monomers were synthesized by the esterification method [13]. 0.99 g of hexadecanol in dichloromethane (25 ml) was mixed with 0.38 g of cyanoacetic acid in ethyl acetate (2.5 ml). The mixture was activated by addition of 0.11 g of 1,4-dimethylaminopyridine and 0.93 g of 1,3-dicyclohexylcarbodiimide in dichloromethane (10 ml). The reaction was carried out for 6 h at room temperature. The products were added to cold diethyl ether in a dropwise manner and the precipitates were filtered and lyophilized.

For the synthesis of poly(hexadecylcyanoacrylate) (PHDCA) by condensation polymerization, 3.1 g of HDCA monomer was dissolved in ethyl alcohol (30 ml) and dichloromethane (5 ml) [18]. Then, formaldehyde solution (37.0%, 0.42 ml) and dimethylamine solution (40.0%, 0.16 ml) were added to the reactant solution. The reaction was carried out for 12 h at room temperature. After the solvent was evaporated, the products were washed with diethyl ether before drying under vacuum. The yield of PHDCA polymer was 91 wt% (2.82 g).

2.4. Preparation of MPNs by the emulsion solvent evaporation method

5 mg of DOX was solubilized in chloroform (5 ml) containing triethylamine (3–5 M in respect to DOX) by sonication for 10 min [19]. Then, 100 mg of PHDCA polymer and 20 mg of magnetic nanocrystal dissolved in chloroform (5 ml) were added to the above solution. This organic phase was added to 1% of PVA (20 ml). After mutual saturation of the organic and the continuous phase, the mixture was emulsified for 10 min under ultrasonification (ULH700S, Ulssohitech) operated at 420 W. After solvent evaporation, the magnetic PHDCA nanoparticles (MPNs) were purified by three cycles of centrifugation at 15 000 rpm and stored under vacuum. To observe the magnetic mobility under magnetic field using epi-fluorescence microscopy, 0.5 mg rhodamine B was encapsulated in the MPNs.

2.5. Preparation of multifunctional MPDCs

The multifunctional MPDCs were prepared by ionic self-assembly of the anionic MPNs and polycationic PEI. 4, 8, 12, 16, 20, 40, 80, 160 and 320 μg PEI dissolved in 1 ml PBS was added to 8 μg ml^{-1} solution of MPNs. The mixture was vortexed for 20 s and gently mixed at 4 °C for 15 min to allow PEI/MPN nanocomplexes (MPDCs). The products were purified by centrifugation at 5000 rpm, lyophilized and stored under vacuum. To investigate magnetic mobility of the MPDCs under external magnetic field using epi-fluorescence microscopy, 0.5 mg ml^{-1} of FITC solution was conjugated with PEI on the surface of MPDCs at room temperature for 12 h. The isothiocyanate group of FITC is exceedingly reactive towards amine groups of PEI [20].

2.6. Magnetic mobility test of MPDCs

MPDCs stained with fluorescent dyes were injected into a borosilicate micro-channel (sq I.D. 500 μm, VitroCom Inc.). The mobility of the MPDCs under a magnetic field (Nd–B–Fe magnet, 0.35 T) was investigated using an epi-fluorescence microscope (Olympus, BX51).

2.7. MR imaging

MR imaging experiments were performed with a 1.5 T clinical MRI instrument with a micro-47 surface coil (Intera, Philips Medical Systems). $T2$ relaxivities ($R2$) of the MPDCs containing magnetic nanocrystals were measured at room temperature by the Carr–Purcell–Meiboom–Gill (CPMG) sequence: TR = 10 s, 32 echoes with 12 ms even echo space, number of acquisition = 1, point resolution of 156 μm × 156 μm, section thickness of 0.6 mm. $R2$ defined as $1/T2$ with units of s^{-1}. The relaxivity coefficient (mM^{-1} s^{-1}) equals the ratio of $R2$ to the MPDC concentration.

2.8. Drug loading contents, entrapment efficiency and drug release kinetics

The total amount of drug in the MPDCs suspension was analysed by drying the sample and dissolving the sample in 5 ml of chloroform. The amount of drug (λ_{max} = 480 nm) in the oil phase was detected by a UV spectrophotometer (Optizen 2120UV, MECASYS Co.). The drug loading contents and entrapment efficiency was calculated by using the following equations:

$$\text{Drug loading contents (\%)} = \frac{\text{weight of drug in nanoparticles}}{\text{weight of prepared nanoparticles}} \times 100$$

$$\text{Entrapment efficiency (\%)} = \frac{\text{weight of drug in nanoparticles}}{\text{weight of injected drug}} \times 100.$$

For the *in vitro* drug release test, 10 mg of MPDCs suspended in 1 ml of PBS (10 mM, pH 7.4) was sealed in a dialysis tube and immersed in 9 ml of PBS at 37 °C. The system was shaken at a moderate speed and the amount of released drug was monitored using a UV spectrophotometeric method.

2.9. Affinity test of the MPDCs against the cancer cell line

Human breast adenocarcinoma MDA-MB-231 cells were obtained from the American Tissue Type Culture (ATCC, Rockville, MD) and cultured in DMEM/F-12 (1:1) media supplemented with 10% (v/v) fetal bovine serum (FBS), 100 U ml^{-1} penicillin, 0.1 mg ml^{-1} streptomycin and 365 μg ml^{-1} L-glutamine at 37 °C in a 5% CO_2-humidified incubator. All culture media were obtained from Gibco (Fisher Scientific, Pittsburgh, PA). We used fluorescence-activated cell sorting (FACS) and MRI to determine the affinity of the DOX-loaded MPNs (DOX-MPNs) and DOX-loaded MPDCs (DOX-MPDCs) to the MDA-MB-231 cells. 1×10^6 cells were incubated with DOX-MPNs and DOX-MPDCs at 37 °C for 4 h in the media described above. The cells were then washed twice with PBS trypsinization and harvested. The collected cells were washed three times with 0.2% FBS and 0.02% NaN_3 in PBS. These samples were re-suspended in 400 μl of 4% paraformaldehyde, and the cell-associated fluorescence was determined by FACS-based analysis of doxorubicin fluorescence using a FACScalibur (Beckton-Dickinson, Mansfield, MA) with the laser operating at 488 nm.

2.10. Cytotoxicity studies

Cell viability was determined in MDA-MB-231 cells maintained in DMEM (Dulbecco's modified eagle's medium) in a 5% CO_2 atmosphere. Cytotoxicity of MPNs and MPDCs was evaluated by measuring the inhibition of cell growth using MTT assay at various concentrations (4.9–625 μg ml^{-1}). In addition, MTT assay was conducted with free DOX, DOX-MPNs and DOX-MPDCs to investigate the cytotoxic efficacy of DOX-MPDCs. The amount of loading contents of DOX was 0.35 μg ml^{-1} as mentioned in section 2.8 (*drug loading contents, entrapment efficiency and drug release kinetics*) and the concentration of DOX was fixed at 0.35 μg ml^{-1} for MTT assay. All treatments were performed on cells seeded in 96-well plates at a cellular density of 4×10^3 cells ml^{-1}. After treatment, the cells were washed and incubated for an additional 72 h. MTT assay was performed using the Cell Proliferation kit (Roche, USA) in triplicate. Cell viabilities were then finally obtained by the ratio of the number of cells treated with free DOX, DOX-MPNs, or DOX-MPDCs to the number of non-treated control cells.

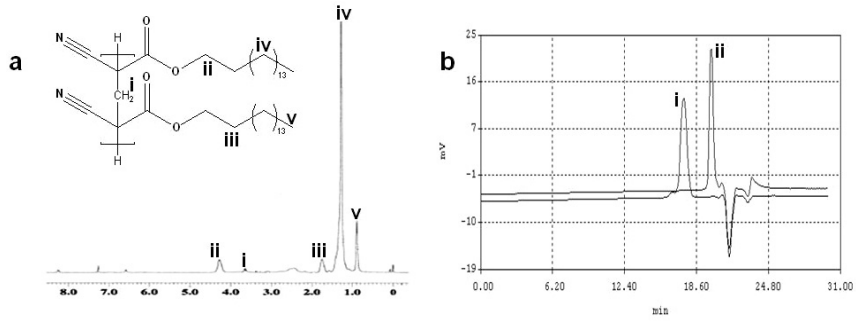

Figure 2. (a) ^{1}H-NMR spectrum of PHDCA polymers and (b) gel permeation chromatography of (i) PHDCA polymers, (ii) HDCA monomers.

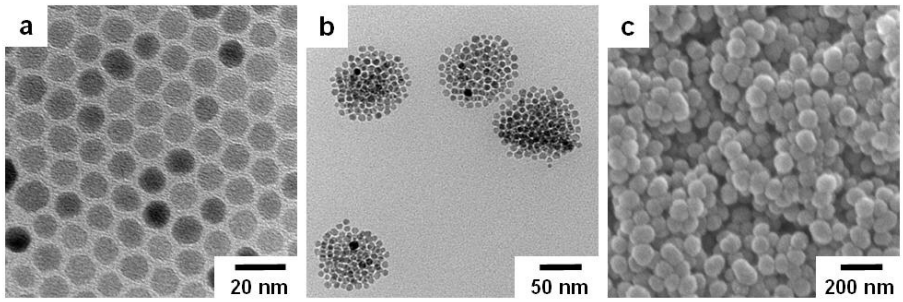

Figure 3. TEM images of (a) magnetic nanocrystals, (b) MPNs and (c) SEM image of MPNs.

2.11. Statistical analysis

All experiments were performed in triplicate and the values were expressed as average ± standard deviation. The statistical evaluation of data was performed by analysis of variance (ANOVA), followed by Tukey's test for comparison of relative $T2$ weight value and cell viability from different groups. $p < 0.05$ was considered to be statistically significant.

2.12. Characterization

The structure of the synthesized PHDCA polymer was confirmed by ^{1}H-NMR spectra (JNM-ECP300, JEOL Ltd), and the molecular weight of the PHDCA was measured using a gel permeation chromatography column (Styragel® HR 2, Waters). Morphology and size distribution were evaluated with a transmittance electron microscope (TEM, JEM-1011, JEOL Ltd) and scanning electron microscope (SEM, JSM-6500F, JEOL Ltd). Size distribution and surface charge of the MPDCs were analysed by laser scattering (ELS-Z, Otsuka electronics). Fourier transform infrared (FT-IR) spectra (Excalibur™ series, Varian Inc.) analysis was used to confirm the characteristic bands of the synthesized nanoparticles. The quantity of magnetic nanocrystals in the MPDCs was determined by a thermogravimetric analyser (SDT-Q600, TA instrument). The saturation of magnetization was evaluated using a vibrating-sample magnetometer (VSM, MODEL-7300, Lakeshore). Surface composition of the MPDCs was investigated by x-ray photoelectron spectroscopy (ESCALAB 220i-XL, VG Scientific Instrument).

3. Results and discussion

Synthesized PHDCA was characterized using a ^{1}H-NMR spectrometer (figure 2(a)) giving δ values of 4.27 (methylene in the α-position to the ester groups), 3.64 (methylene protons of poly(cyanoacrylate)), 1.75 (methylene in the β-position to the ester groups), 1.26 (methylene of hexadecyl chain) and 0.88 (methyl protons of the hexadecyl chain). The molecular weight of the PHDCA was 3900 (Mw), with a low index of polydispersity (1.3) (figure 2(b)).

Using organic solvent, 10.3 ± 0.7 nm of monodisperse magnetic nanocrystals (Fe_3O_4) were synthesized (figure 3(a)). To form the MPNs, magnetic nanocrystals in organic solvent and DOX were simultaneously encapsulated with the synthesized PHDCA using the emulsion solvent evaporation method. Figure 3(b) demonstrates that magnetic nanocrystals are well incorporated in the PHDCA nanoparticles. The prepared MPNs have a uniformly spherical shape and smooth surfaces (figure 3(c)). Furthermore, the narrow size distribution (105.4 ± 10.0 nm) of the MPNs was confirmed by laser scattering.

To evaluate the potential for magnetic drug targeting and the magnetic sensitivity of the MPNs under a magnetic field, the magnetic moment was analysed using a vibrating sample magnetometer. The hysteresis loops of pure magnetic nanocrystals and the MPNs observed at 300 K exhibited superparamagnetic behavior without magnetic hysteresis (figure 4). The saturation of magnetization values of the pure magnetic nanocrystals and the MPNs at 0.9 T were 47.9 and 16.6 emu g^{-1}, respectively. The value for the MPNs was lower than that of the magnetic nanocrystals due to the presence

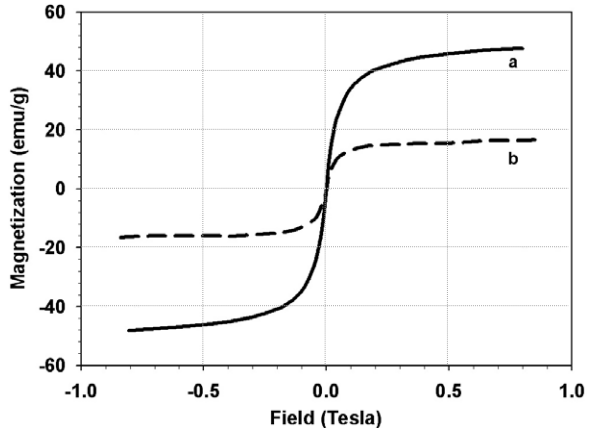

Figure 4. Magnetic hysteresis loops using a vibrating sample magnetometer; (a) magnetic nanocrystals and (b) MPNs.

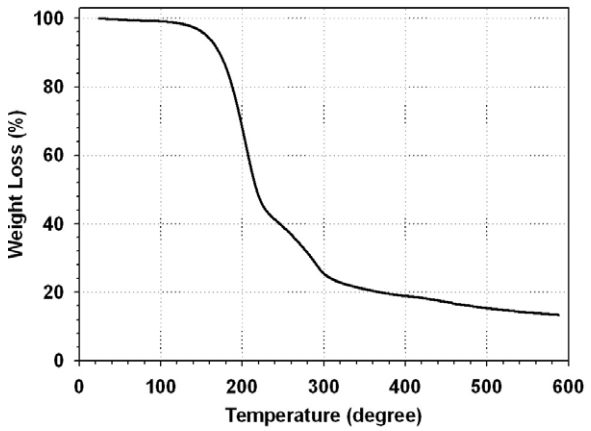

Figure 5. Thermogravimetric curve of MPNs.

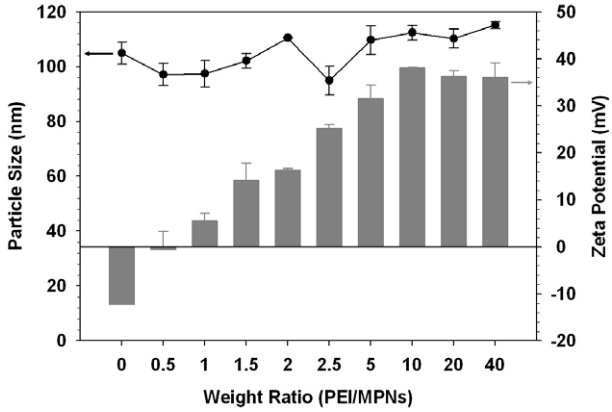

Figure 6. Particle size and zeta potential of the MPNs and the MPDCs according to the PEI/MPNs ratio.

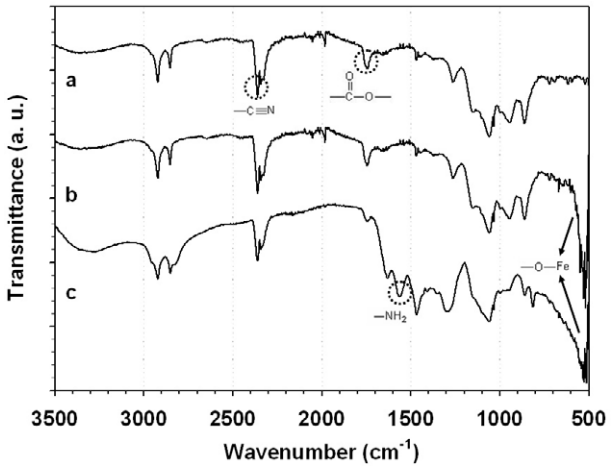

Figure 7. FT-IR spectrum of (a) PHDCA nanoparticles, (b) the MPNs and (c) the MPDCs.

of organic components (PHDCA polymers and DOX). The amount of magnetic nanocrystals encapsulated in the MPNs was determined to be 13.4 wt% using a thermogravimetric analyser (figure 5).

The anionic MPNs were coated with polycationic PEI to enhance cellular uptake efficiency. As shown in figure 6, the zeta potential values of the MPDCs increased from -12.2 ± 4.1 mV to 38.0 ± 0.1 mV as the weight ratio of PEI/MPNs increased. This indicates that there was ionic interaction between the polycationic PEI and the anionic MPNs at the surface of the MPNs. MPDCs showed almost the same particle size and zeta potential values when the ratio of PEI/MPNs was higher than 10. Therefore, the optimal weight ratio of PEI/MPNs was determined to be 10.

The presence of the magnetic nanocrystals and PEI in the MPDCs was confirmed by FT-IR spectra. The characteristic bands of the PHDCA nanoparticles were observed at 2277 cm^{-1} (C≡N) and 1740 cm^{-1} (O–C=O) (figure 7(a)). After encapsulating magnetic nanocrystals into the nanoparticles, a band presented at 550 cm^{-1} (Fe–O), depending on the Fe(II) content in the PHDCA (figure 7(b)). The spectrum of the MPDCs showed characteristic bands at 1600 cm^{-1} (–NH_2) from the primary amine groups of PEI (figure 7(c)).

To further verify the surface modification of the MPDCs, the surface elemental composition of the MPDCs was compared with that of the MPNs using x-ray photoelectron spectroscopy (XPS). The XPS spectra of the MPNs with and without PEI are illustrated in figure 8. The peaks at 282–297, 395–410 and 528–548 eV correspond to the elements of C 1s, N 1s and O 1s, respectively. The relative intensity of the O 1s peak of the MPNs was lower than that of the MPDCs. In addition, the Fe 2p peaks of magnetic nanocrystals at 700–740 eV were not observed in the MPDCs, demonstrating that the MPDCs had a core–shell structure resulting from ionic interaction between PEI and the MPNs.

Magnetic mobility under an external magnetic field was observed as shown in figure 9. The MPDCs well dispersed in PBS of PCR tube without magnet accumulated on the side of the tube within 1 min when a magnet was applied (figures 9(a) and (d)). Epi-fluorescence microscopic images of the MPDCs stained with fluorescence dye (rhodamine B encapsulated in the MPDCs and FITC conjugated with PEI) were also obtained in a rectangular channel of square internal diameter 1.0 mm. When the commercial Nd–Fe–B magnet (0.35 T) was placed on the wall of the channel, the MPDCs accumulated on the wall within 1 min (figures 9(e) and (f)). This demonstrated

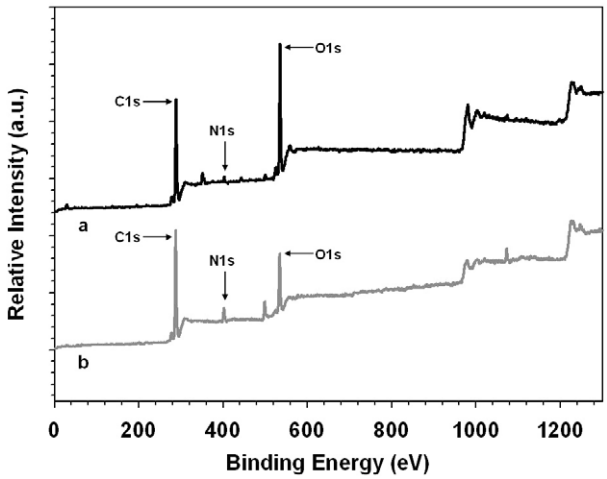

Figure 8. XPS analysis of the surface of (a) the MPNs and (b) the MPDCs.

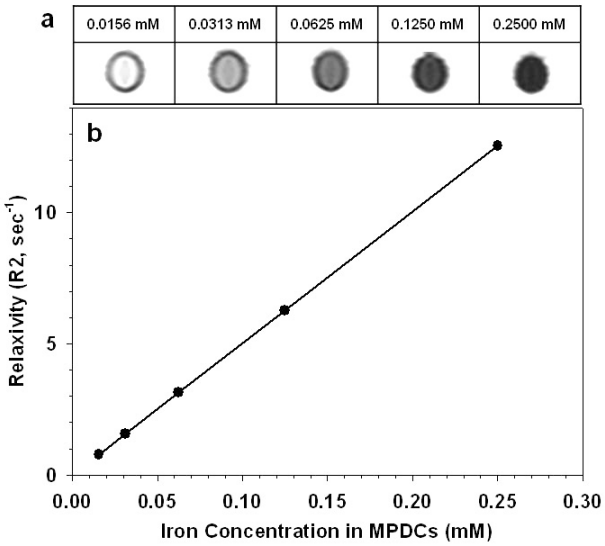

Figure 10. (a) $T2$-weighted MR images of the MPDCs in aqueous solution. (b) Graph of $\Delta R2/R2$ versus the iron concentration in the MPDCs.

that the MPDCs had sufficient sensitivity to external magnetic fields and appeared to have sufficient magnetization to serve as magnetic drug carriers for targeted delivery.

We also investigated the MR contrasting effect of the MPDCs by measuring their $T2$ relaxivity ($R2$) to confirm their utility as MR contrast agents. In the spin–spin relaxation time ($T2$) weighted MR images, the MPDC solution presented as a dark color at high concentrations (figure 10(a)). The relaxivity coefficient of the MPDCs (50.2 mM^{-1} s^{-1}) was about 1.25 times higher compared to that of the nanocrystals (40.3 mM^{-1} s^{-1}) in a previous study (figure 10(b)) [21]. These results demonstrate that the MPDCs have properties suitable for magnetic targeted delivery to cancer cells and real-time monitoring of cancer treatment, despite the presence of the organic components PHDCA polymers and DOX.

The loading contents and entrapment efficiency of DOX in the MPDCs were 3.47 and 77.4 wt%, respectively. An *in vitro* drug release test was performed in triplicate, and the mean value and standard deviation were calculated. The *in vitro* drug release profile of the MPDCs showed a sustained release (figure 11). After 10 days, 82% of the encapsulated DOX was released due to a rapid degradation of PHDCA [22].

The affinity of MPNs and MPDCs to human breast cancer cells was measured using MDA-MB-231 cells. As shown in figure 12, the MDA-MB-231 cells incubated with the DOX-MPDCs demonstrated higher fluorescence intensity by FACS analysis than those incubated with DOX-MPNs and the relative intensity was 16.7 times higher than non-treated control cells. We believe that this enhancement of cell affinity was mainly contributed by the presence of cationic PEI on the MPDCs.

The changes of $T2$-weighted MR signal intensity in cells indicated the potential of cancer detection (figure 13). In figure 13, the MR images of MDA-MB-231 cells treated with

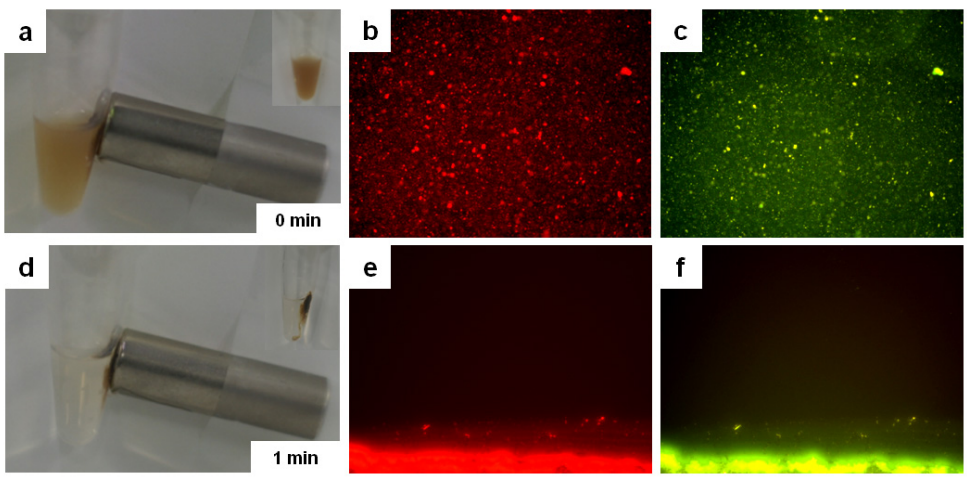

Figure 9. Captured images of (a) dispersed MPDCs in PBS after 0 min and (d) accumulated MPDCs on the side of the tube after 1 min with a magnet. Epi-fluorescence microscopic images of the MPDCs stained with fluorescence dye (rhodamine B encapsulated in the MPDCs and FITC conjugated with PEI). The images in (b) and (c) show MPDCs with no magnetic field while (e) and (f) show MPDCs accumulated on the bottom of the channel with a magnetic field. 1000× magnification.

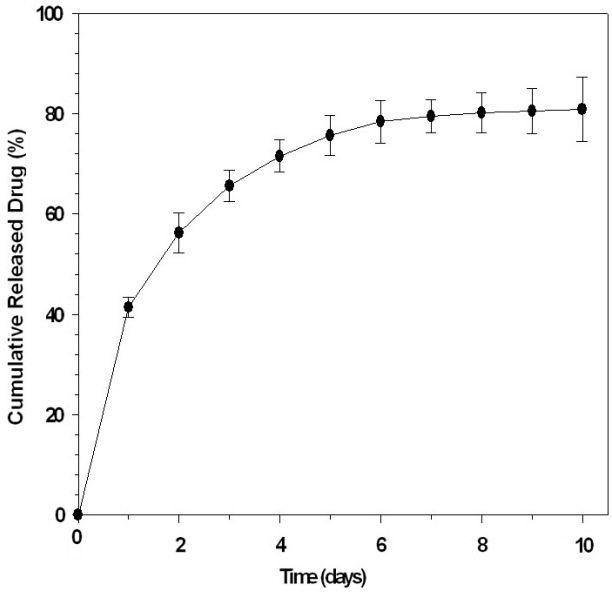

Figure 11. Drug release profile of MPDCs.

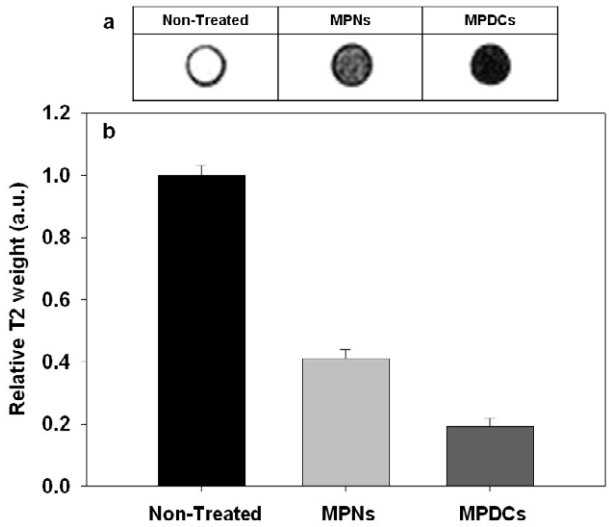

Figure 13. (a) The $T2$-weighted MR images (non-treated; white, MPNs; gray, MPDCs; black) and (b) graph of relative $T2$ weight values for MDA-MB-231 cells.

cationic MPDCs exhibited a dark black color (relative $T2$ weight, $19.2 \pm 2.7\%$) while the one treated with anionic MPNs showed gray color (relative $T2$ weight, $41.0 \pm 2.8\%$). It should be remembered that the MPNs treated cells showed partial enhancement against the MR signal intensity due to non-specific binding. These noteworthy results indicated that cationic MPDCs not only exhibited efficient MR imaging agents but also increased affinity to cancer cells due to enhancement of electrostatic interaction between cationic MPDCs and anionic membrane in MDA-MB-231 cells.

We next determined the *in vitro* cytotoxic activity measured by MTT assay and the results are shown in figure 14. In figure 14(a), the cell viability of MPNs and MPDCs retained over 80% within the concentration range of 4.9–156 μg ml^{-1}. To assess the therapeutic efficacy of the MPDCs, MTT assay was performed with the samples of free DOX, DOX-MPNs and DOX-MPDCs with various DOX concentrations (0.001 37–0.35 μg ml^{-1}) based on the initial DOX concentration (0.35 μg ml^{-1}) in 10 μg ml^{-1} of DOX-MPDCs. In figure 14(b), the DOX-MPDCs showed higher therapeutic efficacy to the DOX-MPNs and free DOX above 0.0055 μg ml^{-1} of DOX concentration, whereas there is similar therapeutic efficacy among three types of samples (free DOX, DOX-MPNs, and DOX-MPDCs) below 0.0055 μg ml^{-1} of DOX concentration. Moreover, the cytotoxicity of DOX-MPNs was significantly less compared with that of the DOX-MPDCs. From the results of cell viability data, the synthesized MPDCs demonstrated that the cationic MPDCs increased

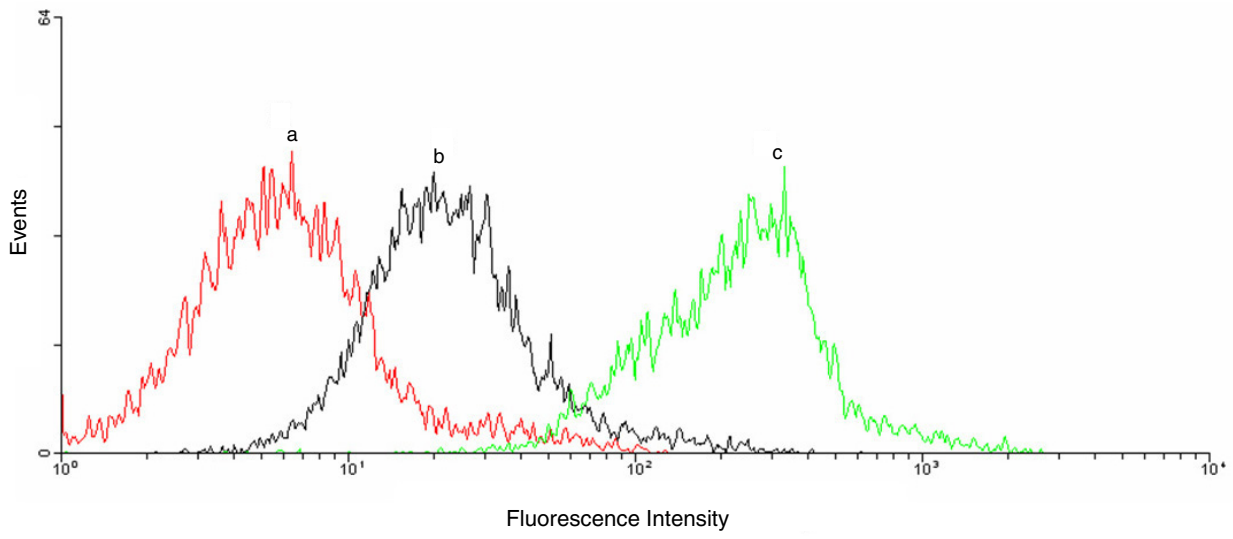

Figure 12. Flow cytometry results of (a) non-treated control cells, (b) MPNs treated cells and (c) MPDCs treated cells; MDA-MB-231 cells. (This figure is in colour only in the electronic version)

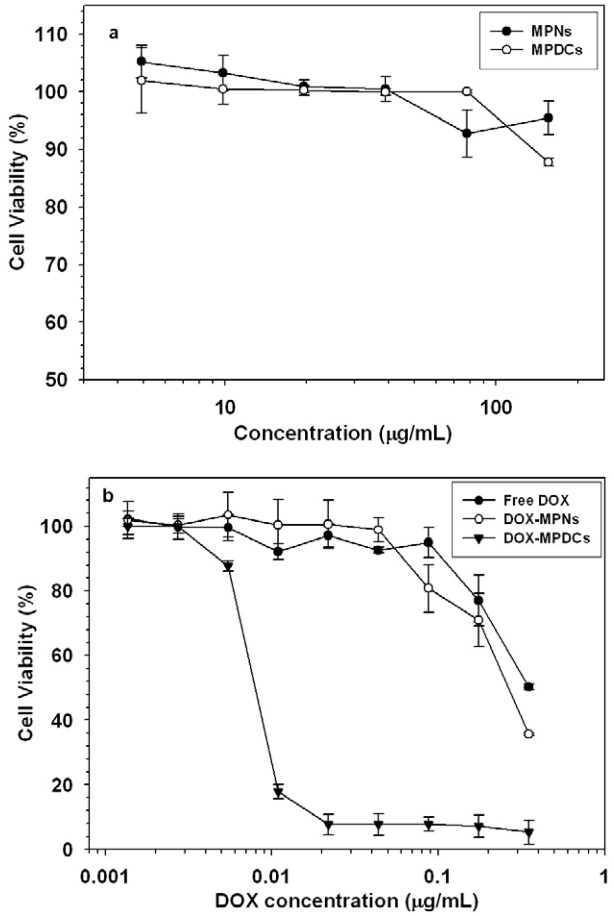

Figure 14. The cell viability test of MDA-MB-231 cells by MTT assay; treated with (a) MPNs and MPDCs at various concentrations of particles, (b) free DOX, DOX-MPNs and DOX-MPDCs at various concentrations of DOX.

the cell affinity with anionic membrane of cancer cells and enhanced uptake into intracellular cytoplasm in parallel with excellent therapeutic efficacy.

4. Conclusion

We successfully synthesized novel MPDCs composed of magnetic nanocrystals and anti-cancer drug encapsulated in PHDCA nanoparticles covered with a PEI layer. The MPDCs demonstrated sufficient magnetic mobility under external magnetic field and ultrasensitivity for simultaneous magnetically targeted drug carriers using MR probes for the detection of cancer. Furthermore, the cationic surface of the MPDCs enhanced the efficiency of cellular uptake by cancer cells. Moreover, the MTT assay results proved that the synthesized MPDCs were nontoxic and the DOX-MPDCs exhibited excellent tumorcidal efficacy. These multifunctional MPDCs can be applied to magnetically targeted drug carriers which also facilitate simultaneous diagnosis by MRI. Further *in vivo* studies are in progress.

Acknowledgments

This work was supported by KOSEF through National Core Research Center for Nanomedical Technology (R15-2004-024-00000-0), Korea Science and Engineering Foundation (KOSEF) grant funded by the Korean government (MOST) (KOSEF 2007-8-1158), the National R&D Program for Cancer Control, Ministry of Health & Welfare, Republic of Korea (0620190-1) and the Yonsei University Research Fund of 2006.

References

[1] Alivisatos P 2004 *Nat. Biotechnol.* **22** 47
[2] Gao X, Yang L, Petros J A, Marshall F F, Simons J W and Nie S 2005 *Curr. Opin. Biotechnol.* **16** 63
[3] Lynch T J *et al* 2004 *New Engl. J. Med.* **350** 2129
[4] Harries M, Ellis P and Harper P 2005 *J. Clin. Oncol.* **23** 7768
[5] Murakami H, Kobayashi M, Takeuchi H and Kawashima Y 2000 *Powder Technol.* **107** 137
[6] Torchilin V P 2000 *Eur. J. Pharm. Sci.* **11** S81
[7] Alexiou C, Arnold W, Klein R J, Parak F G, Hulin P, Bergemann C, Erhardt W, Wagenpfeil S and Lubbe A S 2000 *Cancer Res.* **60** 6641
[8] Senyei A, Wider K and Czerlinski C 1978 *J. Appl. Phys.* **49** 3578
[9] Udrea L E, Strachan N J C, Badescu V and Rotariu O 2006 *Phys. Med. Biol.* **51** 4869
[10] Lee J H *et al* 2007 *Nat. Med.* **13** 95
[11] Yang J, Lee C-H, Park J, Seo S, Lim E-K, Song Y J, Suh J-S, Yoon H-G, Huh Y-M and Haam S 2007 *J. Mater. Chem.* **17** 2695
[12] Sun S, Zeng H, Robinson D B, Raoux S, Rice P M, Wang S X and Li G 2004 *J. Am. Chem. Soc.* **126** 273
[13] Stella B, Arpicco S, Peracchia M T, Desmaele D, Hoebeke J, Renoir M, D'Angelo J, Cattel L and Couvreur P 2000 *J. Pharm. Sci.* **89** 1452
[14] Son K K, Tkach D and Patel D H 2000 *Biochim. Biophys. Acta* **1468** 11
[15] Fewell J G, Matar M, Slobodkin G, Han S O, Rice J, Hovanes B, Lewis D H and Anwer K 2005 *J. Control. Release* **109** 288
[16] Jayakumar R, Prabaharan M, Reis R L and Mano J F 2005 *Carbohydr. Polym.* **62** 142
[17] Zhdanov R I, Podobed O V and Vlassov V V 2002 *Bioelectrochemistry* **58** 53
[18] Brigger I, Chaminade P, Desmaele D, Peracchia M T, D'Angelo J, Gurny R, Renoir M and Couvreur P 2000 *Pharm. Res.* **17** 1124
[19] Dimitrios M, Ryuzo K, Nicola T and Jeffrey A H 2006 *Eur. J. Pharm. Sci.* **29** 120
[20] Jeong J H, Kim S W and Park T G 2003 *J. Control. Release* **93** 183
[21] Song H T, Choi J S, Huh Y M, Kim S J, Jun Y W, Suh J S and Cheon J W 2005 *J. Am. Chem. Soc.* **127** 9992
[22] Peracchia M T, Desmaele D, Couvreur P and D'Angelo J 1997 *Macromolecules* **30** 846